Environmental Science & Technology

Article

pubs.acs.org/est

Reduction in NO_x Emission Trends over China: Regional and Seasonal Variations

Dasa Gu,* Yuhang Wang, Charles Smeltzer, and Zhen Liu†

School of Earth and Atmospheric Sciences, Georgia Institute of Technology, Atlanta, Georgia 30332-0340, United States

Supporting Information

ABSTRACT: We analyzed satellite observations of nitrogen dioxide (NO_2) columns by the Ozone Monitoring Instrument (OMI) over China from 2005 to 2010 in order to estimate the top-down anthropogenic nitrogen oxides (NO_x) emission trends. Since NO_x emissions were affected by the economic slowdown in 2009, we removed one year of abnormal data in the analysis. The estimated average emission trend is 4.01 ± 1.39% yr^{-1}, which is slower than the trend of 5.8−10.8% yr^{-1} reported for previous years. We find large regional, seasonal, and urban-rural variations in emission trends. The average NO_x emission trend of 3.47 ± 1.07% yr^{-1} in warm season (June−September) is less than the trend of 5.03 ± 1.92% yr^{-1} in cool season (October−May). The regional annual emission trends decrease from 4.76 ± 1.61% yr^{-1} in North China Plain to 3.11 ± 0.98% yr^{-1} in Yangtze River Delta and further down to −4.39 ± 1.81% yr^{-1} in Pearl River Delta. The annual emission trends of the four largest megacities, Shanghai, Beijing, Guangzhou, and Shenzhen are −0.76 ± 0.29%, 0.69 ± 0.27%, −4.46 ± 1.22%, and −7.18 ± 2.88% yr^{-1}, considerably lower than the regional averages or surrounding rural regions. These results appear to suggest that a number of factors, including emission control measures of thermal power plants, increased hydro-power usage, vehicle emission regulations, and closure or migration of high-emission industries, have significantly reduced or even reversed the increasing trend of NO_x emissions in more economically developed megacities and southern coastal regions, but their effects are not as significant in other major cities or less economically developed regions.

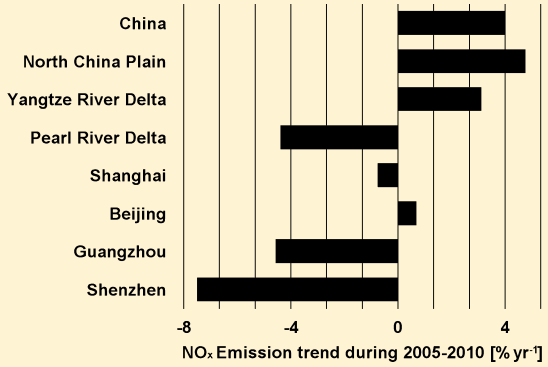

INTRODUCTION

The rapid economic growth in China during the last two decades led to a dramatic increase of energy generation and consumption, which significantly increased nitrogen oxides (NO_x = NO + NO_2) emissions and thereby the tropospheric nitrogen dioxide (NO_2) column densities. Previous studies reported increasing trends varying from 5.8% to 10.8% yr^{-1} for NO_x emissions in the past two decades.[1−3] NO_x emissions in China are mainly driven by power plants and vehicle emissions.[4−6] Recent studies found that NO_x reduction devices have been widely installed in power plants[7] and higher emission standards have been used to regulate motor vehicles in China.[5,8,9] How these control measures affect the NO_x emission trends in China is not yet clear.

The traditional bottom-up inventories of NO_x emissions are estimated using emission source factors and statistical data. They could, therefore, have large uncertainties in China where the emission information is incomplete.[10] Top-down inventories, constrained by satellite observations, could help reduce emission uncertainties.[11,12] Measurements by satellite instruments including Global Ozone Monitoring Experiment (GOME), Scanning Imaging Absorption Spectrometer for Atmospheric Chartography (SCIAMACHY) and Ozone Monitoring Instrument (OMI) have been used to estimate the NO_x emissions in China and the long-term trends from past decade.[1−4,6,12−22] OMI measurements have also been used to estimate NO_x changes from the 2008 Beijing Olympics Games as well as economic recessions and power plant constructions in China in recent years.[7,21,23−26]

In this study, we analyzed OMI observations of NO_2 columns over China from 2005 to 2010 and estimated NO_x emission trends using simulations of a 3-D Regional chEmical trAnsport Model (REAM). As we will discuss, the regional and seasonal differences in NO_x emission trends are very large. In particular, the economically developed Pearl River Delta regions, which include Guangzhou, Shenzhen, and Hong Kong, show a clear decreasing trend. Our study focuses on quantifying these emission trends and explores the factors contributing to the reduction of NO_x emission trends compared to pre-2005 periods and the regional, seasonal, and urban-rural variations in the emission trends.

MATERIALS AND METHODS

The OMI instrument onboard the NASA Aura satellite has a global coverage with a nadir horizontal resolution of 24 × 13

Received: April 22, 2013
Revised: October 7, 2013
Accepted: October 23, 2013
Published: October 23, 2013

km^2, and passes across the equator at about 13:40 local time.[27] Row anomalies in OMI were found in June 2007 and changed over time. We excluded the data in all flagged rows with anomalies from 2005 to 2010 to obtain a consistent data set. In addition, we only use NO_2 column data when cloud fraction is <20% and the column value is greater (by 150%) than the error estimate. [28]

In this study, we calculated tropospheric NO_2 vertical column densities (VCDs) using the KNMI Dutch OMI NO_2 (DOMINO v2.0) retrieval algorithm[29] with a priori profiles from REAM in place of the default KNMI profiles simulated by the coarser-resolution global chemical transport model TM4.[30] We assume that there is no significant trend in tropospheric NO_2 profiles and used REAM simulated monthly mean tropospheric NO_2 profiles of 2007 as a priori profiles to calculate air mass factors (AMFs) for OMI NO_2 retrievals. As such, the derived emission trends are attributed solely to the observed column NO_2 changes and can be compared to previous column-change based studies.[1,18,31] The 3-D REAM model has been applied to investigate a number of tropospheric chemistry and transport problems in various locations over the world.[25,28,32−40] The model used in this study has a horizontal resolution of 70 × 70 km^2 with 21 vertical layers below 10 hPa. The photochemical and dry deposition modules of REAM were adopted from the GEOS-CHEM model[41] with recent updates of kinetics data.[42] Meteorological fields were assimilated using the WRF model constrained by the NCEP reanalysis product. The anthropogenic NO_x and VOCs emissions are obtained from the inventory by Zhang et al.[43] The biomass burning emissions are taken from the Global Fire Emissions Database, Version 2 (GFEDv2.1; available at http://daac.ornl.gov/). The lightning NO_x emission is parametrized as by Choi et al.[44]

Satellite observations of tropospheric NO_2 columns are closely related with surface NO_x emissions due to the relatively short lifetime of NO_x and higher NO_2/NO_x ratios in the lower troposphere.[12,17,45,46] Some studies assumed a constant proportional relationship between satellite tropospheric NO_2 column and surface emissions in estimating NO_x emission trends.[6,12,17,47,48] However, the assumption can have large errors due to the nonlinear feedback of NO_x emissions on photochemistry. Walker et al.[49] and Lamsal et al.[46] reduced this error by establishing a variable linear relationship between changes in NO_x emissions (E) and changes in tropospheric NO_2 columns (Ω):

$$\frac{\Delta E}{E} = \beta \times \frac{\Delta \Omega}{\Omega} \quad (1)$$

where ΔE is the change of NO_x emissions, and $\Delta\Omega$ is the resulting change in simulated tropospheric NO_2 columns, and β is the local emission-to-column sensitivity. Lu and Streets[45] showed the nonlinearity in β, the value of which decreased from 2 to 0.7 during 1996−2010 as NO_x emissions and hence NO_2 concentrations over Indian power plants increased. We computed the β values using REAM for a 15% local emission changes for each grid. Using a smaller (10%) emission perturbation, we obtained essentially the same results. We calculated the mean β values for the year, and warm (June−September) and cool (October−May) seasons, respectively. The change of annual average β as a function of emissions is shown in Figure 1. As surface NO_x emission increases, the value of β decreases from 1.5 to 0.7 as the chemical nonlinearity effect becomes more significant. The spatial distribution of β is shown in Figure S1 of the Supporting Information, SI. Over high NO_x emission regions of eastern China, the annual mean value of β is in the range of 0.7−0.9, implying that relative anthropogenic emission change is 10−30% lower than NO_2 column change. Our β ratios are lower over eastern China than the global model results by Lamsal et al.[46] (SI).

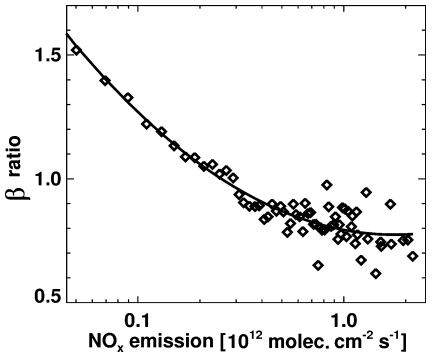

Figure 1. Simulated annual average β values as a function of NO_x emission over China in 2007. The data are binned by NO_x emissions with an interval of 2 × 10^{10} molecules cm^{-2} s^{-1}.

Applying the β ratios to satellite tropospheric NO_2 column observations, we compute the NO_x emission changes from 2005 to 2010. We then estimate the monotonic trends using the Mann-Kendall method with Sen's slope estimator, which is a nonparametric statistical method and has been applied in long-time trend analysis of NO_x, ozone, and other trace gases.[50−56] By using the Mann-Kendall method, we minimize the impacts of seasonal variations and extreme values in the trend analysis. In this study, only statistically significant trend values (using z-test in the Mann-Kendall method) are reported, and the trend uncertainty is given as the 95th percentile confidence interval.

Instead of a linearized trend, we compute in this study the compound annual growth rate, which implicitly assumes exponential emission growth.[2,3] Many previous studies computed a linearized trend over the whole study period, which is normalized to the emission rate in the first year or an average over the study period.[1,13,18−20,56,57] The linearized trend makes it difficult to compare emission rate changes since the normalization year varies among the studies. Furthermore, the implicit assumption of a linearized trend that the per-year (relative) growth rate decreases gradually during the study period cannot be easily justified. A linearized trend normalized to the emission rate in the first year tends to overestimate the growth rate if emission increases and underestimate the reduction rate if emission decreases.

For regional trend analysis, we define 4 regions (Figure S2 of the SI): Northeast China (NEC, 29°−41° N and 108.75°−123.25° E), North China Plain (NCP, 34°−40° N and 113°−120° E), Yangtze River Delta (YRD, 30°−32.5° N and 118°−122° E) and Pearl River Delta (PRD, 22°−23.5° and 112.5°−114° E). On the basis of correlation analysis of monthly trends, we define June to September as warm season and October to May as cool season in the seasonal analysis.

Impact of Economic Recession. The Chinese economy went into a recession in late 2008 after the summer Olympic Games and lasted for ∼1 year. The total import and export statistics[58] (Figure 2) showed continuing growth from 2005 to the middle of 2008, a sudden drop in 2009 coinciding with the recession, and a recovery in 2010. Similarly, the average OMI tropospheric NO_2 VCDs over China (Figure 2) showed

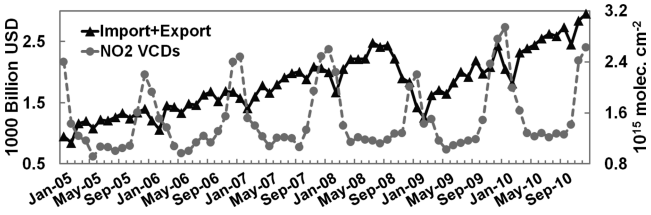

Figure 2. Total national import and export in China,[58] and monthly average tropospheric NO_2 VCDs over China during 2005−2010.

corresponding changes. Previous studies found that the economic recession of 2009 had a significant effect on anthropogenic NO_x emissions.[20,23] To properly characterize the trends of NO_x emissions and make comparison with previous studies, we choose to exclude one year data from August 2008 to July 2009 in this work. Including the economic recession period in analysis would result in a decrease of the annual-mean NO_x emission trend over China from 4.01% to 3.87% yr^{-1}.

RESULTS AND DISCUSSION

Seasonal and Spatial Variations. Figure 2 shows significant seasonal variations in OMI tropospheric NO_2 columns with a maximum in cool season and a minimum in warm season, reflecting in part a shorter photochemical lifetime in warm season. We examine the seasonal variation of NO_x emission trend by month and VCDs (Figure S3 of the SI). While the emission trend is mostly positive generally in a range of 3−5% yr^{-1}, we also find negative emission trend down to −7% yr^{-1} in warm season for high NO_2 VCD regions, indicating potentially significant seasonal variation of NO_x emission trend in high emission regions.

We show in Figure 3 the distributions of the annual-mean OMI-derived NO_x emission trends as well as the averages for warm and cool seasons. The most striking spatial feature is the decreasing trend of NO_x emissions over the PRD region. A closer inspection shows another region, in the vicinity of YRD (near Shanghai and nearby Jiangsu and Zhejiang provinces), also has generally lower increasing emission trends or even decreasing trends. In general, NO_x emissions have lower increases over affluent and economically developed coastal regions than less developed and relatively poor inland areas.

The spatial distributions of emission trends for warm and cool seasons also follow a similar pattern. However, the average trend of 3.47 ± 1.07% yr^{-1} in warm season is lower than 5.03 ± 1.92% yr^{-1} in cool season. In addition, the warm season distribution shows a much larger negative trend region surrounding PRD than in the cool season. The growth rate of NO_x emissions is in general lower in southern China than northern China, likely reflecting the more extensive consumption of hydropower (e.g., the Three Gorges Dam) generated electricity in the warm season in southern China.[59] We will examine this factor in the next section.

Regional Trend Variations. We examine here annual trends in different regions to understand the large regional variations (Figure 3). Table 1 shows that more economically developed and more affluent PRD and YRD regions have lower emission trends than NCP and NEC.

Our estimated national annual compound growth rate of 4.01 ± 1.39% yr^{-1} for NO_x emission is lower than previously estimated NO_x emission trends of 5.8−10.8% yr^{-1} or tropospheric NO_2 column trends of 7.3−29% yr^{-1} during 1996−2006. The previous estimates of emission and NO_2 column trends were summarized in Tables 1 and S1 (SI), respectively. As we discussed previously, a linearized growth rate estimate tends to have a higher increase and lower decrease than a compound growth rate and the difference is about 10% for our study period (Table S2 in SI). More important is the scaling factor of column to emission trend ratio, β, in the range of 0.7−0.9 over high NO_x emission regions of eastern China, which leads to 10−30% lower relative emission changes than column NO_2 changes (eq 1, and Tables S2 and S3 of the SI). After taking into account of methodological difference (20−40%) from previous studies, the trend of NO_x emissions still appears to have slowed from the rates in 1996−2006. A recent study estimated a bottom-up NO_x emission trend of 5.4% yr^{-1} over China during 2007−2010,[60] which is consistent with our finding. However, we do not have adequate information to compare bottom-up emission trend estimates with the top-down trends in detail. Instead, we focus our discussion on the major factors that could significantly affect NO_x emission trends.

An important policy factor relevant to emission trends during 2005−2010 is the Energy Saving and Emission Reduction Policy. The policy was implemented in the 11th Five-Year Plan (2006−2010) in order to reduce energy consumption per unit

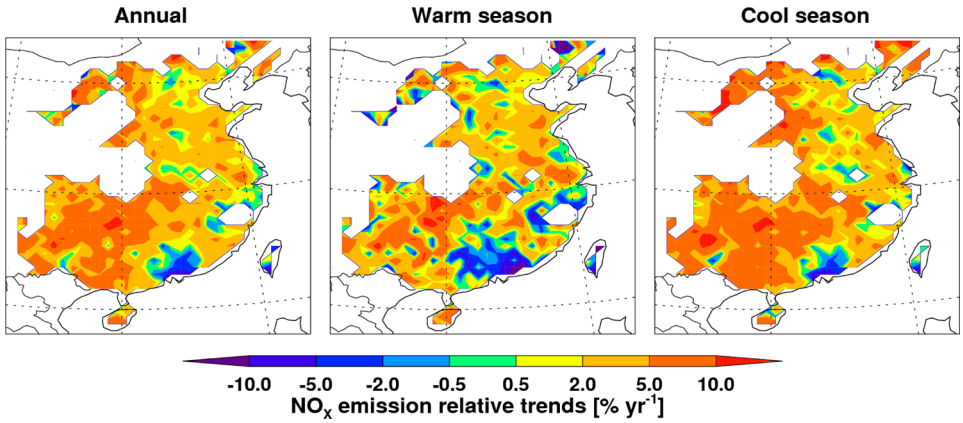

Figure 3. Annual and seasonal (warm and cool) relative NO_x emission trends over China during 2005−2010. Warm season is June−September and cool season is October−May.

Table 1. Comparison of National and Regional Trends of NO_x Emissions over China between This and Previous Studies[a]

period	region	annual trend (% yr^{-1})	method and references
2005−2010	China	4.01 ± 1.39	OMI - REAM; compound rate; this work
	Northeast China	4.55 ± 1.36	
	North China Plain	4.76 ± 1.61	
	Yangtze River Delta	3.11 ± 0.98	
	Pearl River Delta	−4.39 ± 1.81	
1996−2002	China	5.8	GOME − CMAQ; compound rate; Kurokawa el al.[2]
	North China Plain	7.5	
	Yangtze River Delta	12.3	
1997−2006	China	7.3	GOME & SCIAMACHY - IMAGES CTM; compound rate; Stavrakou et al.[3]
2000−2005	Center East China	10.8	GOME & SCIAMACHY − CMAQ/REAS; linearized rate; He et al.[1]
	Yangtze River Delta	8.2	

[a]Additional top-down emission trend estimates are listed in Table S1 in Supporting Information.

of gross domestic product (GDP) by 20% and major pollutant emissions by 10% during the plan period.[61] The Chinese government also put it into the performance evaluation of provincial governors from 2007. Power plants, petroleum industries, iron and steel industries were regulated due to their high-energy consumption and pollutant emissions.

An important technology improvement is NO_x emission reduction of thermal power generation. It is required by the Chinese Air Pollutants Emission Standards of Thermal Power Stations (GB13223−2003). During 2006−2010, 76.83 million kilowatt (kW) thermal power generation capacity of small stations was closed, out of a total of 900 million kW total thermal power generation capacity.[62,63] At the end of 2007, nearly 10% of the thermal power generation capacity had applied the Denitration ($DeNO_x$) systems, in which 96% used the Selective Catalytic Reduction (SCR) (nearly 90% reduction efficiency) and 4% used Selective Non-Catalytic Reduction (SNCR) (40% ∼ 70% reduction efficiency).[64,65] It was estimated that 3 million tons of thermal power generated NO_x emissions could be reduced by the end of 2010, which accounts 28% of total thermal power generated NO_x during the period.[66] The installation of DeNOx systems was initially concentrated in the vicinity of the 4 largest megacities, the impact of which will be discussed in the next section.

These factors alone, however, do not necessarily explain the regional variations in Table 1, although power plants in PRD and YRD regions are likely to be preferentially fitted with $DeNO_x$ systems due to stronger enforcements and potentially higher public awareness of environmental issues among the more affluent population.[67] One likely important factor is the increasing use of hydro and nuclear power, and it is estimated that hydropower capacity increased by 13% yr^{-1} in China from 2005 to 2010.[59] The larger increase of hydropower mainly benefits southern China where it is generated.[68,69]

Among large NO_x emission regions, PRD is the only one showing a significant decreasing trend of NO_x emissions. The specific reasons are not entirely clear. As the most economically developed region in China, PRD, is also the first region that made substantial efforts to reduce major pollutant emissions to improve local environments, which appeared to be successful. In addition to using hydro and nuclear power[68,70,71] and implementing more stringent vehicle emission standards in major cities, the rapid closure of energy-inefficient industries and relocation of high-energy consumption industries to inland province could be a major factor.[72−77] Increasing labor costs, the economic recession, and government policies encouraging technology upgrades all appeared to contribute to the observed decreasing emission trend in that region.

Megacity Trends and Urban-Rural Difference. The disparity of NO_x emission trends as a function of economic development is more evident for megacities. In Figure 4, we show estimated NO_x emission trends for the 4 largest megacities, Shanghai, Beijing, Guangzhou, and Shenzhen, all of which have >10 million in population and > $;100 billion in GDP per year. The annual NO_x relative emission trends of these cities are −0.76 ± 0.29%, 0.69 ± 0.27%, −4.46 ± 1.22% and −7.18 ± 2.88% yr^{-1}, respectively. Guangzhou and Shenzhen, which have negative emission trends, are located in the PRD region. In comparison, we also show in the figure the next 8 major cities ranked by their GDP values in 2009.[78] The annual relative emission trends of the 4 largest megacities are less than 1% or negative, while the other cities have larger positive trends. Also shown in Figure 4 are the emission trends for the nearby rural regions defined as the surrounding eight grids of a city grid. While the difference between urban and rural regions are relatively small for the other 8 cities, the rural regions surrounding the 4 largest megacities show consistently higher emission trends than the cities, although the rural trends of the 4 largest megacities are still less than the other cities in general.

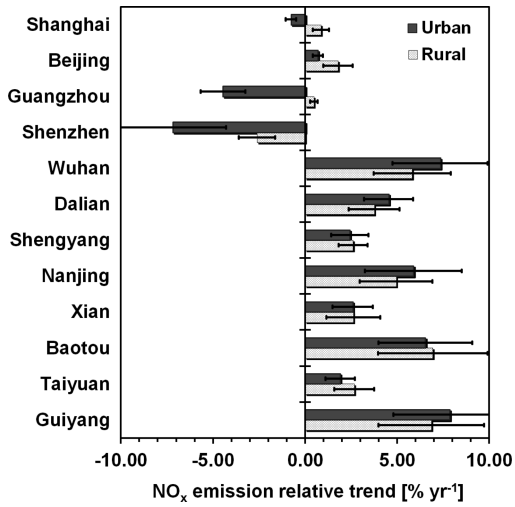

Figure 4. Estimated NO_x emission trends for urban and surrounding rural areas of 12 cities ranked by GDP. The error bars show the 95th percentile confidence intervals.

As mentioned before, DeNO$_x$ systems were gradually applied to thermal power plants in China during 2006−2010, and power plants in the 4 largest megacities were preferentially fitted these systems due to stronger enforcements and higher public awareness.[67,79,80] The use of SCR and SNCR technologies could have significantly reduced NO$_x$ emissions in the 4 largest megacities in past few years, but we expect that the benefit for further emission reduction will taper off where most power plants have these technologies. However, we may begin to see NO$_x$ emission reduction in other cities in future as the use of DeNO$_x$ systems increases in other regions.

Due to rapid economic development, the numbers of on-road vehicles have increased significantly in all Chinese cities. In cities like Shanghai where new vehicle licenses are limited, the number of on-road vehicles did decrease proportionally since residents often bought vehicle licenses from surrounding regions. The fact that the 4 largest megacities showed lower emission trends is likely due to the much stricter vehicle emission standards and more effective enforcement than the other cities.[5,8,9] The Euro 3 standard was implemented in 2005, and the Euro 4 standard was implemented in 2008. Guangzhou changed buses and taxi cabs to liquefied petroleum gas (LPG) engines, starting from 2004. By 2007, 80% of buses and all 16 000 taxis cabs in Guangzhou were fitted with LPG engines which had lower NO$_x$ emissions than gasoline engines.[81] The extensive development of metro railways is another reason. The fractions of public transportation by metro railways are 37% in Shanghai, 23% in Beijing, and 15% in Guangzhou by 2009, which are much higher than the other cities.[78]

Lastly, the 4 largest megacities are more willing to close small energy-inefficient industries or relocate high energy-consumption industries due to a combination of urban development needs and public environmental concerns. The economic loss from losing these industries can be easily recovered by development of new business in these cities. The Olympics Games in Beijing in 2008, the Asian Game in Guangzhou in 2010, and the World Expo in Shanghai in 2010 likely precipitated the migration of high-emission industries away from these cities.

Implications. We find that using the compound growth rate and accounting for the nonlinear ratio of relative column NO$_2$ to emission trend are important for estimating NO$_x$ emission trends using satellite column observations. Our estimation of an annual anthropogenic NO$_x$ emission increase of 4.01 ± 1.39% yr^{-1} is significantly lower than previous estimates of 5.8−10.8% yr^{-1} in China over the period of 1996−2006, suggesting a slowdown of NO$_x$ emissions over China in more recent years. The average NO$_x$ emission trend is larger in cool season (5.03 ± 1.92% yr^{-1}) than in warm season (3.47 ± 1.07% yr^{-1}), reflecting in part potentially more extensive usage of hydropower in warm season. The regional difference is even larger. More economically developed and affluent PRD and YRD regions have lower (than NCP) or negative emission trends. The NO$_x$ emission trends of the 4 largest megacities, Shanghai, Beijing, Guangzhou, and Shenzhen are −0.76 ± 0.29%, 0.69 ± 0.27%, −4.46 ± 1.22%, and −7.18 ± 2.88% yr^{-1}, considerably lower than the trends of 2−7.8% yr^{-1} of the other 8 major cities. The difference is also apparent when comparing urban emission trends to surrounding regions in these cities. The rural regions surrounding the 4 largest megacities show consistently higher emission trends than the cities, while the difference between urban and rural regions are relatively small for the other 8 major cities.

The lower emission increases (and even decreases) in economically developed regions reflect successful implementation of environmental regulations from direct emission control to industry changes. Looking into the future, it is likely that some of these control measures will be gradually implemented in other megacities and economically developed regions (other than PRD and YRD), which will help reduce emissions growth in those cities and broader regions in China. The implementation of these measures will likely be slower over rural and less economically developed regions of China, and the rate of emission increase will likely remain high as economy in those regions continues to develop.

■ ASSOCIATED CONTENT

Ⓢ Supporting Information

(1) Summary of NO$_2$ column trends in previous study results (Table S1); (2) β value distribution (Figure S1); (3) Relative emission and VCD trend estimates in this work (Table S2 and S3, Figure S2 and S3). This material is available free of charge via the Internet at http://pubs.acs.org.

■ AUTHOR INFORMATION

Corresponding Author

*Phone: (404)333-9654; e-mail: dasagu@gatech.edu.

Present Address

[†]Combustion Research Facility, Sandia National Laboratories, Livermore, CA, U.S.

Notes

The authors declare no competing financial interest.

■ ACKNOWLEDGMENTS

This work was supported by the National Science Foundation Atmospheric Chemistry and NASA ACMAP Programs. We thank Kebin He for his suggestion of the impact of DeNO$_x$ system installation on megacities.

■ REFERENCES

(1) He, Y.; Uno, I.; Wang, Z.; Ohara, T.; Sugirnoto, N.; Shimizu, A.; Richter, A.; Burrows, J. P. Variations of the increasing trend of tropospheric NO$_2$ over central east China during the past decade. *Atmos. Environ.* **2007**, *41* (23), 4865−4876.

(2) Kurokawa, J.; Yumimoto, K.; Uno, I.; Ohara, T. Adjoint inverse modeling of NO$_x$ emissions over eastern China using satellite observations of NO$_2$ vertical column densities. *Atmos. Environ.* **2009**, *43* (11), 1878−1887.

(3) Stavrakou, T.; Muller, J. F.; Boersma, K. F.; De Smedt, I.; van der A, R. J. Assessing the distribution and growth rates of NO$_x$ emission sources by inverting a 10-year record of NO$_2$ satellite columns. *Geophys. Res. Lett.* **2008**, *35* (10), 5.

(4) Shi, C. N.; Fernando, H. J. S.; Wang, Z. F.; An, X. Q.; Wu, Q. Z. Tropospheric NO$_2$ columns over East Central China: Comparisons between SCIAMACHY measurements and nested CMAQ simulations. *Atmos. Environ.* **2008**, *42* (30), 7165−7173.

(5) Wang, H. K.; Fu, L. X.; Zhou, Y.; Du, X.; Ge, W. H. Trends in vehicular emissions in China's mega cities from 1995 to 2005. *Environ. Pollut.* **2010**, *158* (2), 394−400.

(6) Zhang, Q.; Streets, D. G.; He, K.; Wang, Y.; Richter, A.; Burrows, J. P.; Uno, I.; Jang, C. J.; Chen, D.; Yao, Z.; Lei, Y. NO$_x$ emission trends for China, 1995−2004: The view from the ground and the view from space. *J. Geophys. Res.-Atmos.* **2007**, *112* (D22), 18.

(7) Li, C.; Zhang, Q.; Krotkov, N. A.; Streets, D. G.; He, K. B.; Tsay, S. C.; Gleason, J. F. Recent large reduction in sulfur dioxide emissions from Chinese power plants observed by the Ozone Monitoring Instrument. *Geophys. Res. Lett.* **2010**, 37.

(8) Saikawa, E.; Kurokawa, J.; Takigawa, M.; Borken-Kleefeld, J.; Mauzerall, D. L.; Horowitz, L. W.; Ohara, T. The impact of China's vehicle emissions on regional air quality in 2000 and 2020: A scenario analysis. *Atmos. Chem. Phys.* **2011**, *11* (18), 9465−9484.
(9) Wu, Y.; Wang, R. J.; Zhou, Y.; Lin, B. H.; Fu, L. X.; He, K. B.; Hao, J. M. On-road vehicle emission control in Beijing: Past, present, and future. *Environ. Sci. Technol.* **2011**, *45* (1), 147−153.
(10) Streets, D. G.; Bond, T. C.; Carmichael, G. R.; Fernandes, S. D.; Fu, Q.; He, D.; Klimont, Z.; Nelson, S. M.; Tsai, N. Y.; Wang, M. Q.; Woo, J. H.; Yarber, K. F., An inventory of gaseous and primary aerosol emissions in Asia in the year 2000. *J. Geophys. Res.-Atmos.* **2003**, *108*, (D21).
(11) Lamsal, L. N.; Martin, R. V.; van Donkelaar, A.; Steinbacher, M.; Celarier, E. A.; Bucsela, E.; Dunlea, E. J.; Pinto, J. P., Ground-level nitrogen dioxide concentrations inferred from the satellite-borne ozone monitoring instrument. *J. Geophys. Res.-Atmos.* **2008**, *113*, (D16).
(12) Martin, R. V.; Jacob, D. J.; Chance, K.; Kurosu, T. P.; Palmer, P. I.; Evans, M. J., Global inventory of nitrogen oxide emissions constrained by space-based observations of NO_2 columns. *J. Geophys. Res.-Atmos.* **2003**, *108*, (D17).
(13) Ghude, S. D.; Van der A, R. J.; Beig, G.; Fadnavis, S.; Polade, S. D. Satellite derived trends in NO_2 over the major global hotspot regions during the past decade and their inter-comparison. *Environ. Pollut.* **2009**, *157* (6), 1873−1878.
(14) Han, K. M.; Song, C. H.; Ahn, H. J.; Park, R. S.; Woo, J. H.; Lee, C. K.; Richter, A.; Burrows, J. P.; Kim, J. Y.; Hong, J. H. Investigation of NO_x emissions and NO_x-related chemistry in East Asia using CMAQ-predicted and GOME-derived NO_2 columns. *Atmos. Chem. Phys.* **2009**, *9* (3), 1017−1036.
(15) Kunhikrishnan, T.; Lawrence, M. G.; von Kuhlmann, R.; Richter, A.; Ladstatter-Weissenmayer, A.; Burrows, J. P. Analysis of tropospheric NO_x over Asia using the model of atmospheric transport and chemistry (MATCH-MPIC) and GOME-satellite observations. *Atmos. Environ.* **2004**, *38* (4), 581−596.
(16) Ma, J. Z.; Richter, A.; Burrows, J. P.; Nuss, H.; van Aardenne, J. A. Comparison of model-simulated tropospheric NO_2 over China with GOME-satellite data. *Atmos. Environ.* **2006**, *40* (4), 593−604.
(17) Richter, A.; Burrows, J. P.; Nuss, H.; Granier, C.; Niemeier, U. Increase in tropospheric nitrogen dioxide over China observed from space. *Nature* **2005**, *437* (7055), 129−132.
(18) van der A, R. J.; Eskes, H. J.; Boersma, K. F.; van Noije, T. P. C.; Van Roozendael, M.; De Smedt, I.; Peters, D.; Meijer, E. W. Trends, seasonal variability and dominant NO_x source derived from a ten year record of NO_2 measured from space. *J. Geophys. Res.-Atmos.* **2008**, *113* (D4), 12.
(19) van der A, R. J.; Peters, D.; Eskes, H.; Boersma, K. F.; Van Roozendael, M.; De Smedt, I.; Kelder, H. M. Detection of the trend and seasonal variation in tropospheric NO_2 over China. *J. Geophys. Res.-Atmos.* **2006**, *111* (D12), 10.
(20) Schneider, P.; van der A, R. J. A global single-sensor analysis of 2002−2011 tropospheric nitrogen dioxide trends observed from space. *J. Geophys. Res.* **2012**, *117* (D16), D16309.
(21) Zhang, Q.; Geng, G. N.; Wang, S. W.; Richter, A.; He, K. B. Satellite remote sensing of changes in NO_x emissions over China during 1996−2010. *Chin. Sci. Bull.* **2012**, *57* (22), 2857−2864.
(22) Wang, S. W.; Zhang, Q.; Streets, D. G.; He, K. B.; Martin, R. V.; Lamsal, L. N.; Chen, D.; Lei, Y.; Lu, Z. Growth in NO_x emissions from power plants in China: Bottom-up estimates and satellite observations. *Atmos. Chem. Phys.* **2012**, *12* (10), 4429−4447.
(23) Lin, J.; Nielsen, C. P.; Zhao, Y.; Lei, Y.; Liu, Y.; McElroy, M. B. Recent changes in particulate air pollution over China observed from space and the ground: Effectiveness of emission control. *Environ. Sci. Technol.* **2010**, *44* (20), 7771−7776.
(24) Witte, J. C.; Schoeberl, M. R.; Douglass, A. R.; Gleason, J. F.; Krotkov, N. A.; Gille, J. C.; Pickering, K. E.; Livesey, N., Satellite observations of changes in air quality during the 2008 Beijing Olympics and Paralympics. *Geophys. Res. Lett.* **2009**, *36*.
(25) Yang, Q.; Wang, Y.; Zhao, C.; Liu, Z.; Gustafson, W. I.; Shao, M. NO_x emission reduction and its effects on ozone during the 2008 Olympic Games. *Environ. Sci. Technol.* **2011**, *45* (15), 6404−6410.
(26) Zhang, Q.; Streets, D. G.; He, K. B. Satellite observations of recent power plant construction in Inner Mongolia, China. *Geophys. Res. Lett.* **2009**, *36*, 5.
(27) Levelt, P. F.; Hilsenrath, E.; Leppelmeier, G. W.; van den Oord, G. H. J.; Bhartia, P. K.; Tamminen, J.; de Haan, J. F.; Veefkind, J. P. Science objectives of the ozone monitoring instrument. *IEEE Trans. Geosci. Remote Sens.* **2006**, *44* (5), 1199−1208.
(28) Zhao, C.; Wang, Y. Assimilated inversion of NO_x emissions over east Asia using OMI NO_2 column measurements. *Geophys. Res. Lett.* **2009**, *36* (6), L06805.
(29) Boersma, K. F.; Eskes, H. J.; Dirksen, R. J.; van der A, R. J.; Veefkind, J. P.; Stammes, P.; Huijnen, V.; Kleipool, Q. L.; Sneep, M.; Claas, J.; Leitão, J.; Richter, A.; Zhou, Y.; Brunner, D. An improved tropospheric NO_2 column retrieval algorithm for the Ozone Monitoring Instrument. *Atmos. Meas. Tech.* **2011**, *4* (9), 1905−1928.
(30) Heckel, A.; Kim, S. W.; Frost, G. J.; Richter, A.; Trainer, M.; Burrows, J. P. Influence of low spatial resolution a priori data on tropospheric NO_2 satellite retrievals. *Atmos. Meas. Tech.* **2011**, *4* (9), 1805−1820.
(31) Russell, A. R.; Valin, L. C.; Cohen, R. C. Trends in OMI NO_2 observations over the United States: Effects of emission control technology and the economic recession. *Atmos. Chem. Phys.* **2012**, *12* (24), 12197−12209.
(32) Choi, Y.; Wang, Y.; Zeng, T.; Cunnold, D.; Yang, E. S.; Martin, R.; Chance, K.; Thouret, V.; Edgerton, E., Springtime transitions of NO_2, CO, and O_3 over North America: Model evaluation and analysis. *J. Geophys. Res.-Atmos.* **2008**, *113*, (D20).
(33) Choi, Y.; Wang, Y. H.; Yang, Q.; Cunnold, D.; Zeng, T.; Shim, C.; Luo, M.; Eldering, A.; Bucsela, E.; Gleason, J., Spring to summer northward migration of high O_3 over the western North Atlantic. *Geophys. Res. Lett.* **2008**, *35*, (4).
(34) Choi, Y.; Wang, Y. H.; Zeng, T.; Martin, R. V.; Kurosu, T. P.; Chance, K., Evidence of lightning NO_x and convective transport of pollutants in satellite observations over North America. *Geophys. Res. Lett.* **2005**, *32*, (2).
(35) Gray, B. A.; Wang, Y. H.; Gu, D. S.; Bandy, A.; Mauldin, L.; Clarke, A.; Alexander, B.; Davis, D. D. Sources, transport, and sinks of SO_2 over the equatorial Pacific during the Pacific Atmospheric Sulfur Experiment. *J. Atmos. Chem.* **2011**, *68* (1), 27−53.
(36) Liu, Z.; Wang, Y.; Gu, D.; Zhao, C.; Huey, L. G.; Stickel, R.; Liao, J.; Shao, M.; Zhu, T.; Zeng, L.; Amoroso, A.; Costabile, F.; Chang, C. C.; Liu, S. C. Summertime photochemistry during CAREBeijing-2007: RO_x budgets and O_3 formation. *Atmos. Chem. Phys.* **2012**, *12* (16), 7737−7752.
(37) Liu, Z.; Wang, Y. H.; Gu, D. S.; Zhao, C.; Huey, L. G.; Stickel, R.; Liao, J.; Shao, M.; Zhu, T.; Zeng, L. M.; Liu, S. C.; Chang, C. C.; Amoroso, A.; Costabile, F. Evidence of reactive aromatics as a major source of peroxy acetyl nitrate over China. *Environ. Sci. Technol.* **2010**, *44* (18), 7017−7022.
(38) Wang, Y. H.; Choi, Y. S.; Zeng, T.; Ridley, B.; Blake, N.; Blake, D.; Flocke, F., Late-spring increase of trans-Pacific pollution transport in the upper troposphere. *Geophys. Res. Lett.* **2006**, *33*, (1).
(39) Zhao, C.; Wang, Y.; Choi, Y.; Zeng, T., Summertime impact of convective transport and lightning NO_x production over North America: Modeling dependence on meteorological simulations. *Atmos. Chem. Phys.* **2009**, *9*, (13).
(40) Zhao, C.; Wang, Y. H.; Zeng, T. East China plains: A "basin" of ozone pollution. *Environ. Sci. Technol.* **2009**, *43* (6), 1911−1915.
(41) Bey, I.; Jacob, D. J.; Yantosca, R. M.; Logan, J. A.; Field, B. D.; Fiore, A. M.; Li, Q. B.; Liu, H. G. Y.; Mickley, L. J.; Schultz, M. G. Global modeling of tropospheric chemistry with assimilated meteorology: Model description and evaluation. *J. Geophys. Res.-Atmos.* **2001**, *106* (D19), 23073−23095.
(42) Sander, S. P.; Abbate, J.; Barker, J. R.; Burkholder, J. B.; Friedl, R. R.; Golden, D. M.; Huie, R. E.; Kolb, C. E.; Kurylo, M. J.; Moortgat, G. K.; Orkin, V. L.; Wine, P. H. Chemical Kinetics and Photochemical

Data for Use in Atmospheric Studies, Evaluation No 17. J. P., 10−6. Jet Propulsion Laboratory: Pasadena, CA, 2011.
(43) Zhang, Q.; Streets, D. G.; Carmichael, G. R.; He, K. B.; Huo, H.; Kannari, A.; Klimont, Z.; Park, I. S.; Reddy, S.; Fu, J. S.; Chen, D.; Duan, L.; Lei, Y.; Wang, L. T.; Yao, Z. L. Asian emissions in 2006 for the NASA INTEX-B mission. *Atmos. Chem. Phys.* **2009**, *9* (14), 5131−5153.
(44) Choi, Y.; Wang, Y.; Yang, Q.; Cunnold, D.; Zeng, T.; Shim, C.; Luo, M.; Eldering, A.; Bucsela, E.; Gleason, J. Spring to summer northward migration of high O_3 over the western North Atlantic. *Geophys. Res. Lett.* **2008**, *35* (4), L04818.
(45) Lu, Z.; Streets, D. G. Increase in NO_x emissions from indian thermal power plants during 1996−2010: Unit-based inventories and multisatellite observations. *Environ. Sci. Technol.* **2012**, *46* (14), 7463−7470.
(46) Lamsal, L. N.; Martin, R. V.; Padmanabhan, A.; van Donkelaar, A.; Zhang, Q.; Sioris, C. E.; Chance, K.; Kurosu, T. P.; Newchurch, M. J. Application of satellite observations for timely updates to global anthropogenic NO_x emission inventories. *Geophys. Res. Lett.* **2011**, *38* (5), L05810.
(47) Kaynak, B.; Hu, Y.; Martin, R. V.; Sioris, C. E.; Russell, A. G. Comparison of weekly cycle of NO_2 satellite retrievals and NO_x emission inventories for the continental United States. *J. Geophys. Res.-Atmos.* **2009**, 114.
(48) Wang, Y. X.; McElroy, M. B.; Martin, R. V.; Streets, D. G.; Zhang, Q.; Fu, T. M. Seasonal variability of NO_x emissions over east China constrained by satellite observations: Implications for combustion and microbial sources. *J. Geophys. Res.-Atmos.* **2007**, *112* (D6), 19.
(49) Walker, T. W.; Martin, R. V.; van Donkelaar, A.; Leaitch, W. R.; MacDonald, A. M.; Anlauf, K. G.; Cohen, R. C.; Bertram, T. H.; Huey, L. G.; Avery, M. A.; Weinheimer, A. J.; Flocke, F. M.; Tarasick, D. W.; Thompson, A. M.; Streets, D. G.; Liu, X. Trans-Pacific transport of reactive nitrogen and ozone to Canada during spring. *Atmos. Chem. Phys.* **2010**, *10* (17), 8353−8372.
(50) Buckley, S. M.; Mitchell, M. J. Improvements in urban air quality: Case studies from New York State, U.S.A. *Water Air Soil Pollut.* **2011**, *214* (1−4), 93−106.
(51) Carslaw, D. C. Evidence of an increasing NO_2/NO_x emissions ratio from road traffic emissions. *Atmos. Environ.* **2005**, *39* (26), 4793−4802.
(52) Cattani, G.; di Bucchianico, A. D.; Dina, D.; Inglessis, M.; Notaro, C.; Settimo, G.; Viviano, G.; Marconi, A. Evaluation of the temporal variation of air quality in Rome, Italy from 1999 to 2008. *Ann. Ist. Super. Sanita* **2010**, *46* (3), 242−253.
(53) Grant, A.; Yates, E. L.; Simmonds, P. G.; Derwent, R. G.; Manning, A. J.; Young, D.; Shallcross, D. E.; O'Doherty, S. A five year record of high-frequency in situ measurements of non-methane hydrocarbons at Mace Head, Ireland. *Atmos. Meas. Tech.* **2011**, *4* (5), 955−964.
(54) Shon, Z. H.; Kim, K. H.; Song, S. K. Long-term trend in NO_2 and NO_x levels and their emission ratio in relation to road traffic activities in East Asia. *Atmos. Environ.* **2011**, *45* (18), 3120−3131.
(55) Sicard, P.; Dalstein-Richier, L.; Vas, N. Annual and seasonal trends of ambient ozone concentration and its impact on forest vegetation in Mercantour National Park (South-eastern France) over the 2000−2008 period. *Environ. Pollut.* **2011**, *159* (2), 351−362.
(56) Sicard, P.; Mangin, A.; Hebel, P.; Mallea, P. Detection and estimation trends linked to air quality and mortality on French Riviera over the 1990−2005 period. *Sci. Total Environ.* **2010**, *408* (8), 1943−1950.
(57) Hilboll, A.; Richter, A.; Burrows, J. P. Long-term changes of tropospheric NO_2 over megacities derived from multiple satellite instruments. *Atmos. Chem. Phys. Discuss.* **2012**, *12* (12), 31767−31828.
(58) *Brief Statistics on China's Import & Export*; Ministry of Commerce, China: http://english.mofcom.gov.cn/statistic/statistic.html, 2011.
(59) Yu, X.; Qu, H. The role of China's renewable powers against climate change during the 12th Five-Year and until 2020. *Renew. Sust. Energy Rev.* **2013**, *22* (0), 401−409.
(60) Zhao, B.; Wang, S. X.; Xu, J. Y.; Fu, K.; Klimont, Z.; Hao, J. M.; He, K. B.; Cofala, J.; Amann, M. NO_x emissions in China: Historical trends and future perspectives. *Atmos. Chem. Phys. Discuss.* **2013**, *13* (6), 16047−16112.
(61) Wang, S.; Hao, J. Air quality management in China: Issues, challenges, and options. *J. Environ. Sci.* **2012**, *24* (1), 2−13.
(62) Report on energy saving and emission reduction of electric power Industry during 2010 and the 11th Five-Year Plan; State Electritiy Regulatory Commission of China: China, http://www.serc.gov.cn/jggg/201208/W020111026348300590384.doc, 2011.
(63) Zhao, Y.; Zhang, J.; Nielsen, C. P. The effects of recent control policies on trends in emissions of anthropogenic atmospheric pollutants and CO_2 in China. *Atmos. Chem. Phys.* **2013**, *13* (2), 487−508.
(64) CAEPI. China Development Report on Desulfurization and Denitration Industry of Power Plant in 2010. China Environmental Protection Industry 2011, (7).
(65) Liang, Z. Y.; Ma, X. Q.; Lin, H.; Tang, Y. T. The energy consumption and environmental impacts of SCR technology in China. *Appl. Energy* **2011**, *88* (4), 1120−1129.
(66) CAEPI. China Development Report on Desulphurization and Denitration Industries in Power Plants in 2007. China Environmental Protection Industry, 2008, (6).
(67) Dong Huang, F. Z., Wang, S. Study on the Flue Gas Denitrification Cost Estimation of Coal-fired Power Plant During the "Twelfth Five-Year Plan" Period of China. *Energy Technology and Economics* **2012**, *24*, (4).
(68) Lei, X. M., *IEEE Market Design and Operational Experience with Generation and Transmission of the Three-Gorges Hydroelectric Power Station*; IEEE: New York, 2005; p 31−35.
(69) McCormack, G. Water margins—Competing paradigms in China. *Crit. Asian Stud.* **2001**, *33* (1), 5−30.
(70) ShenM. D.; LuK. L.Soc Francaise Energie N.Development of nuclear power in Guangdong Province, People's Republic of China*Topnux '96: Economic Nuclear Power for the 21st Century, Vols 1 and 2: Economic Nuclear Power for the 21st Century: Towards the New Generation of Reactors*19966778
(71) Wu, Z. X.; Siddiqi, T. A. The role of nuclear-energy in reducing the environmental impacts of China energy use. *Energy* **1995**, *20* (8), 777−783.
(72) Huang, H.; Wei, Y. H. D. Spatial-temporal patterns and determinants of foreign direct investment in China. *Erdkunde* **2011**, *65* (1), 7−23.
(73) Ferraro, G.; Brans, M. Trade-offs between environmental protection and economic development in China's fisheries policy: A political analysis on the adoption and implementation of the Fisheries Law 2000. *Nat. Resour. Forum* **2012**, *36* (1), 38−49.
(74) Tang, S. Y.; Lo, C. W. H.; Fryxell, G. E. Governance reform, external support, and environmental regulation enforcement in rural China: The case of Guangdong province. *J. Environ. Manage.* **2010**, *91* (10), 2008−2018.
(75) Xie, J. A. *Researches on Application Conditions of Grads Theory and Industrial Transfer in the Eastern Developed Provinces*; M D Forum: Allawah NSW, 2010; pp 303−310.
(76) Yang, Y. Q.; Yu, H. S., *The Empirical Study on the Environmental Impact of Two Typical Trade Growth Pattern: Comparison Based on 1992−2008 Emissions Data of Zhejiang and Guangdong Provinces*; Aussino Acad Publ House: Marrickville, 2010; pp 849−856.
(77) Zheng, F. H.; Qin, S. C. *Environmental Pollution, Environmental Performance of Government and Public Satisfaction: An Empirical Study on Guangdong Province in 2007*; Intellectual Property Publ House: Haidian District, 2009; pp 394−397.
(78) Statistics, C. N. B. o.. *China Statistical Yearbook 2010*; China Statistics Press: Beijing, 2010.
(79) Yang, W. J.; Zhou, Z. J.; Zhou, J. H.; Hongkun, L. V.; Liu, J. Z.; Cen, K. F. Application of hybrid coal reburning/SNCR processes for

NO_x reduction in a coal-fired boiler. *Environ. Eng. Sci.* **2009**, *26* (2), 311−317.
(80) Zhang, L.-j. Energy optimization of SCR coal-fired power plant. *Shanxi Energy Conserv.* **2010**, *3*, 3.
(81) Report on Environmental Quality in Guangzhou 2007; Guangzhou Environmental Protection Angency: Guangzhou, http://www.gzepb.gov.cn/root43/gov/200810/t20081020_4192.htm, 2008.